

## Interaction of hydrogen with magnetism in the $Y_{0.4}Gd_{0.6}H_x$ alloy

P. Vajda

*Laboratoire des Solides Irradiés, CNRS, Ecole Polytechnique, F-91128 Palaiseau, France*

O. J. Zogal

*Institute of Low-Temperature and Structure Research, Polish Academy of Sciences, PL-50950 Wroclaw, Poland*

(Received 26 October 1999)

The magnetic properties of the system  $Y_{0.4}Gd_{0.6}H(D)_x$ , in the concentration range  $0 \leq x \leq 0.25$ , have been determined through electrical resistivity measurements between 1.35 and 300 K. The paramagnetic spin-disorder resistivity  $\rho_m^0$  decreases with increasing H concentration  $x$ , as well as the amplitudes of the antiferromagnetic and ferromagnetic transitions; though the values of the transition temperatures themselves,  $T_N = 192$  K and  $T_C = 80$  K, are hardly affected by hydrogen. No low-temperature solid solution  $\alpha^*$  phase is formed, in accord with the empirical observation relating its existence to the value of the interlayer turn angle between two basal planes in the prevailing magnetic modulation along the  $c$  axis. The introduced hydrogen precipitates as  $GdH_2$ , superimposing an additional magnetic transformation at 3.6 K and interfering with the spin-wave spectrum of the alloy at low temperatures.

The study of yttrium-rare earth ( $R$ ) alloys, with Y playing the role of a diluent for the heavy hcp magnetic rare earths, has a long tradition. Thus, they were, in particular, employed to show how the interlayer turn angle  $\omega_i$  for the various  $c$ -axis-modulated magnetic phases depended on the de Gennes factor,  $\xi = (g_J - 1)^2 J(J + 1)$ , of the alloy (see, e.g., Ref. 1 for a review). More recently, these observations were related, *via* the structural  $c/a$  ratios of these alloys, to the specific shape of the Fermi surface, in particular to their nesting or webbing features.<sup>2</sup> Another only recently appreciated, characteristic property is their ability to absorb large amounts of hydrogen and, therefore, to have the latter as an additional factor for structural and electronic modifications. A (by now) well-known example is the phenomenon of the hydride “switchable mirrors” driven by the H-induced metal-insulator transition in  $R$  films, whose optical gap and hence the color are controlled by alloying.<sup>3</sup> A general review of the physical properties of binary  $R$ -H systems was given a few years ago by one of the authors.<sup>4</sup>

The present investigation, concerning the  $Y_yGd_{1-y}$  system, has been partly motivated by the results obtained by us previously on  $Y_yTb_{1-y}H_x$  alloys,<sup>5</sup> which had shown a certain correlation between the hydrogen solubility at low temperatures (in the  $\alpha^*$  phase) and the ( $y$  dependent) helicity of the manifesting magnetic structures *via* the Fermi-surface topology. It was, in fact, expected that the higher de Gennes factor  $\xi$  and the related smaller interlayer turn angle  $\omega_i$  of Y-Gd alloys compared to Y-Tb alloys, were unfavorable factors for the occurrence of the  $\alpha^*$  phase in the former.<sup>6</sup> A further support for this argumentation was the very recent direct observation by positron annihilation of Fermi-surface webbing in certain Gd-Y alloys exhibiting helical antiferromagnetic (AF) configurations.<sup>7</sup> We had therefore decided to study the alloy system  $Y_yGd_{1-y}H_x$  with  $y = 0.4$ , in order to investigate the influence of hydrogen in a Gd-concentration range close to the limit where both ferromagnetic (FM) and spiral configurations were present.<sup>1</sup>

Early work on nonhydrogenated  $Y_yGd_{1-y}$  alloys included magnetization measurements in the range  $0 \leq y \leq 0.3$  by Thoburn *et al.*<sup>8</sup> and by Bagguley *et al.*,<sup>9</sup> for  $0.36 \leq y \leq 0.94$ , and electrical resistivity measurements by Hennephof<sup>10</sup> and by Sugawara<sup>11</sup> in the concentration range  $0 \leq y \leq 0.3$  and  $y = 0.97 - 0.99$ , respectively. The first qualitative neutron-diffraction experiments establishing the prevailing magnetic structures were performed by Child and Cable<sup>12</sup> in the domain  $0.2 \leq y \leq 0.9$ , complemented later by a detailed magnetic structure determination on single crystals in the multicritical region around  $y = 0.3$  by Bates *et al.*<sup>13</sup> More recently, Foldeaki *et al.*,<sup>14</sup> have studied the modification of crystal-field anisotropy by Y, through susceptibility measurements in the range  $0 \leq y \leq 0.67$ . And, finally, we have already mentioned the positron annihilation study by Fretwell *et al.*,<sup>7</sup> clearly observing the relation between helicity and Fermi-surface webbing in  $Y_{0.38}Gd_{0.62}$ . As concerns the binary systems with hydrogen, we refer to the general review article<sup>4</sup> and to the specific studies of the Y-H  $\alpha^*$  phase<sup>15</sup> and of Gd-H in the two-phase ( $\alpha + \beta$ ) region.<sup>16</sup>

$20 \times 1 \text{ mm}^2$  specimens of 150–250  $\mu\text{m}$  thickness were cut from cold-worked and electropolished  $Y_{0.4}Gd_{0.6}$  foils prepared by the Ames Laboratory (Ames, Iowa). The starting materials were nominally 99.99% Y and 99.97% Gd, with the main metallic impurities: Y ( $>1$  at ppm)–27 Fe, 12 W, 7.5 Cu, 6 Ce, 3.7 Sc, 2.3 Tb, 1.5 Pr, 1.3 Cr; Gd ( $>2$  at ppm)–200 W, 38 Fe, 11 Ta, 10 Al, 5 Si, 4 Na, 3.2 Ni, 2.2 Cu. The foils were provided with four spot-welded Pt contacts for the electrical measurements and then degassed in a quartz furnace at 700–750 °C in a vacuum of  $<10^{-6}$  Torr before hydrogen loading. One thus annealed and one nonannealed pristine  $Y_{0.4}Gd_{0.6}$  sample were employed as base for comparison. Hydrogen was introduced at 500 °C homogenizing for 8 h (for details of the procedure, see, e.g., Ref. 4). The obtained concentrations (to  $\pm 0.015$ ) were  $0_{\text{non-ann}}$ ,  $0_{\text{ann}}$ , 0.05, 0.10, 0.15, 0.20, and 0.25 H and, in view of a possible isotope effect, 0.07 D and 0.10 D.

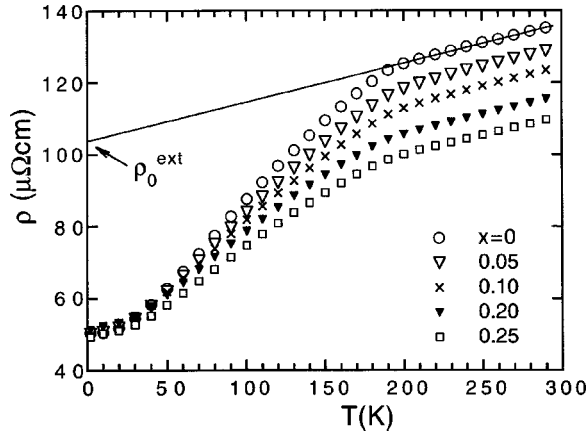


FIG. 1. Temperature dependence of the electrical resistivity in the  $Y_{0.4}Gd_{0.6}H_x$  system, for five selected concentrations  $x$ ;  $\rho_{\text{ext}}^0$  is the phonon resistivity in the paramagnetic range extrapolated to 0 K (see text).

The electrical measurements on up to seven samples simultaneously were done by the classical four-point dc method, in the range 1.35–300 K, with a relative measuring precision on a  $(\rho, T)$  couple of  $10^{-4}$ , corresponding to a sensitivity of better than  $10^{-8} \Omega \text{ cm}$  in our experiments. The absolute precision on the resistivity data, mainly due to the uncertainty of the sample shape factors, is of the order of a few %.

#### High-temperature region

A global view of the resistivity of the  $Y_{0.4}Gd_{0.6}H(D)_x$  system in the whole studied temperature range is presented in Fig. 1 on a series of selected hydrogen concentrations,  $x$ . One notes an essentially invariable residual resistivity,  $\rho_{\text{res}} \sim 50 \mu\Omega \text{ cm}$ , a break near 190 K indicating the Néel temperature given as  $T_N = 196 \text{ K}$  by neutron diffraction,<sup>12</sup> and a rather parallel phonon resistivity for all samples in the paramagnetic range above  $T_N$ , with a slope of  $0.11 \mu\Omega \text{ cm/K}$  at 250–300 K. On the other hand, the slope below  $T_N$ , in relation to the spin-disorder contribution, decreases with increasing  $x$  quite regularly. Table I contains the above and other significant numerical information on all measured specimens, showing especially no notable isotope effect. (Note the roughly 10% lower  $\rho_{\text{res}}$  for the unannealed pristine alloy, indicating a possible contamination by residual air during the annealing procedure, but which apparently does not affect the magnetic characteristics.)

The practically constant  $\rho_{\text{res}}$  is the first and most direct demonstration of the absence of a low-temperature  $\alpha^*$  phase. Hydrogen in solid solution would have led to an increasing  $\rho_{\text{res}}$  [with a parallel shift of the whole  $\rho(T)$  curve], such as observed in binary  $\alpha^*$ - $YH_x$  (Ref. 15) and also in the  $Y_{0.9}Tb_{0.1}H_x$  alloy, but not in  $Y_{0.2}Tb_{0.8}H_x$  where hydrogen precipitated at once as a dihydride (see Ref. 5). This seems to conform with the above-mentioned empirical rule<sup>5,6</sup> that the existence of a low- $T$   $\alpha^*$  phase was limited to systems where the interlayer turn angle of the modulated AF configuration was close to its maximum value  $\omega_i \sim 50 \text{ deg}$ : in the present alloy, Child and Cable<sup>12</sup> have measured a  $\omega_i \sim 25 \text{ deg}$ , itself close to the border for the existence of a helical type of

TABLE I. Specimen characteristics of the alloy system  $Y_{0.4}Gd_{0.6}H(D)_x$ .

$x$	$\rho_{\text{res}}^a$	$d\rho/dT^b$	$\rho_{\text{ext}}^0$	$\rho_m^0$	$d\rho/dT$ (120 K)	$T_N$ (K)	$T_C$ (K)
0 <sub>non-a</sub>	44.38	0.108	97.22	52.84	0.44	192.0	79.0
0 <sub>ann</sub>	50.35	0.106	104.45	54.10	0.44	192.5	79.5
0.05	50.23	0.112	96.44	46.20	0.40	191.0	80.0
0.07D	49.85	0.112	93.95	44.10	0.39	191.0	80.0
0.10	50.93	0.114	90.48	39.55	0.36	190.5	79.5
0.10D	50.47	0.112	91.60	41.13	0.37	191.0	79.5
0.15	51.17	0.114	86.22	35.05	0.33	191.0	79.5
0.20	51.23	0.109	83.78	32.55	0.32	190.5	79.5
0.25	49.00	0.108	78.55	29.55	0.30	190.0	80.0

<sup>a</sup>All  $\rho$  values are in  $\mu\Omega \text{ cm}$ .

<sup>b</sup>All derivatives are in  $\mu\Omega \text{ cm/K}$ .

magnetism in view of the limiting value for its  $c/a$  ratio,  $c/a(Y_{0.4}Gd_{0.6}) = 1.582$ , related to an electronic topological transition and corresponding to the extreme diameter of the Fermi surface.<sup>2</sup> On the other hand, it is reassuring that the (nonmagnetic) Y, possessing an  $\alpha^*$  phase, exhibits webbing features which would correspond to a magnetic modulation with an  $\omega_i = 49.5 \text{ deg}$ .<sup>17</sup>

We have determined the magnetic contribution to resistivity  $\rho_m^0$  by subtracting the residual resistivity from the extrapolated phonon part in the paramagnetic region to 0 K:  $\rho_m^0 = \rho_{\text{ext}}^0 - \rho_{\text{res}}$ , and shown graphically in Fig. 1 for the pure alloy as an example. The values for  $\rho_m^0$  are given in Table I, together with the slopes of the specimens in the magnetically ordered range below  $T_N$ , taken here at 120 K—far enough from any “accidents” (see below).

We note a qualitatively similar decrease with increasing  $x$  for these related parameters, in view of the same mechanism acting upon them. Thus, the spin-disorder resistivity in the paramagnetic region can be expressed (see, e.g., Ref. 1) as  $\rho_m^0 = (\hbar k_F / 4\pi z) (m^* \Gamma / e \hbar^2)^2 (g_J - 1)^2 J(J+1)$ . As has already been suggested in Ref. 5, the role of hydrogen will be to act mainly through a weakening exchange interaction  $\Gamma$ , caused by pumping off conduction electrons, while the simultaneous decrease of the conduction electron number per atom  $z$  will be partially compensated by that of the Fermi wave vector  $k_F$ . The de Gennes factor,  $\xi = (g_J - 1)^2 J(J+1)$ , will not be affected, as it is essentially  $4f$ -ion dependent. It appears, thus, that the  $T$ -dependent spin-disorder resistivity,  $\rho_m = \rho_m^0 [1 - \langle \mathbf{S} \rangle^2 / S(S+1)]$ , where  $S$  are the  $4f$ -electron spins (cf. Ref. 1), does not contain other  $x$ -sensitive terms than  $\rho_m^0$  itself.

Figure 2 presents a clearer view of the  $T$  dependence of the resistivity above 20 K, for three typical concentrations, via a differentiated plot. Indeed, we not only have here a preciser picture of the region around  $T_N$ , permitting us to determine a slight  $x$ -dependent decrease of its value (see Table I) by using the maximum of the second derivative. But, in addition, one notes a peak near 80 K superimposed upon the linear  $\rho$  variation with  $T$  in this range, which seems to be a manifestation of the Curie temperature,  $T_C$ , signaled by Child and Cable<sup>12</sup> at 84 K. An enlarged detailed view in

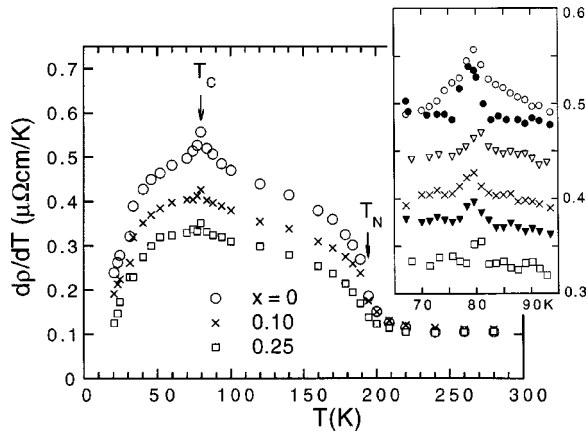


FIG. 2. Resistivity derivatives through the whole  $T$  range above 20 K, for three selected H concentrations, showing the transitions at  $T_C$  and  $T_N$ . The inset is an enlarged view around  $T_C$ , for a series of typical  $x$  values:  $\circ$  is  $0_{\text{ann}}$ ,  $\bullet$  is  $0_{\text{non-ann}}$ ,  $\nabla$  is 0.05,  $\times$  is 0.10,  $\blacktriangledown$  is 0.15,  $\square$  is 0.25 H/unit.

the  $T_C$  area (inset in Fig. 2) shows that the value of  $T_C$  is rather  $x$  independent, oscillating between 79 and 80 K, but its amplitude is clearly diminishing with growing hydrogen contents. Thus, it seems that the Y-Gd interaction, which is maximal at our concentration  $y=0.4$  according to the effective moment determinations by Foldeaki *et al.*,<sup>14</sup> is not modified by hydrogen as expressed through the value of  $T_C$ ; it is only the concentration of the contributing Gd ions (measured *via* the peak amplitude at  $T_C$ ) which appears to be reduced. It is also worth mentioning that the transition at  $T_C$  is broadened in the case of the annealed H-free specimen when compared to the nonannealed cold-rolled one (indicated by filled circles in the inset of Fig. 2); it looks as if the criticality of the transition were somewhat inhibited by the impurities introduced in the anneal and/or by the reduction of texture. Interestingly, the inverse effect had taken place in the  $\text{Y}_{0.2}\text{Tb}_{0.8}$  alloy, where the transition at  $T_C$  was *only* visible in the annealed specimen.<sup>5</sup> It is possible that the smaller interlayer turn angle at  $T_C$  (just before turning zero),  $\omega_{f'} = 14$  deg in the case of  $\text{Y}_{0.4}\text{Gd}_{0.6}$  (as compared to the  $\omega_{f'} = 24$  deg of  $\text{Y}_{0.2}\text{Tb}_{0.8}$ ), related to the higher de Gennes factor  $\xi$  (see Ref. 1), confers a higher stability to the ferromagnetic structure in the present alloy.

#### Low-temperature region

Figure 3 shows the low- $T$  part (below 20 K) of the resistivity derivatives for the same samples as in the inset of Fig. 2. The striking feature in this plot is the appearance, upon the addition of hydrogen, of a shoulder which grows into a clear structure peaking at  $T=3.6$  K. In view of its absence in the H-free alloy, it seems obvious to attribute this peak to the antiferromagnetic dihydride,  $\text{GdH}_2$ , and its temperature to the AF  $T_N^{\text{GdH}_2}$ . This seems very small when compared to the  $T_N^{\text{GdH}_2} = 18.5$  K measured in the bulk dihydride<sup>18</sup> but is not unreasonable when recalling the two-phase system  $\text{GdH}_z$  with  $0 \leq z \leq 2$  (Ref. 16). There, a second, low- $T$ , hump was appearing in the AF region, for small  $z$  values, peaking, e.g., near 4 K for  $z=0.3$ : it was ascribed to the interaction be-

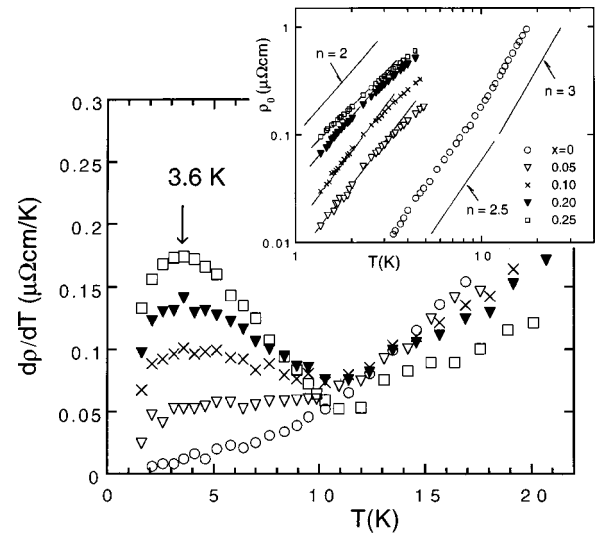


FIG. 3. Same as Fig. 2, in the low- $T$  region, showing the growth of the  $\text{GdH}_2$  peak at  $T_N^{\text{GdH}_2} = 3.6$  K. Inset: temperature dependence of the intrinsic resistivity,  $\rho_0 = \rho_{\text{tot}} - \rho_{\text{res}}$ ; in a double-logarithmic plot, showing the decreasing power  $n$  of the  $T^n$  variation, with increasing  $x$ .

tween the FM Gd domains and the AF domains of  $\text{GdH}_2$  (affecting its spin-wave spectrum) caused by a proximity effect.<sup>16</sup>

The situation in the H-doped alloys can also be considered as that of oversized fcc  $\text{GdH}_2$  domains surrounded by an hcp host lattice under pressure. Now it is known (Ref. 1, for example) that the magnetic ordering temperatures are generally decreasing with increasing pressure due to the changes induced in the magnetic anisotropy energy via magnetostriction. It should be interesting, in this context, to analyze the magnetic structure of our system by neutron diffraction and, specifically, the role of hydrogen in the low- $T$  configuration.

One can also try and look at the low-temperature region where the resistivity behavior is governed by the spin-wave excitation. Such a plot is presented in a double-logarithmic form in the inset of Fig. 3 where we are showing the intrinsic (i.e., here principally the magnetic) resistivity,  $\rho_0 = \rho_{\text{tot}} - \rho_{\text{res}}$ , for a series of specimens. The hydrogen-free alloy exhibits, up to  $\sim 10$  K, a  $T^{2.5}$  dependence turning over into a  $T^3$  dependence at higher temperatures. This is reasonable for a canted ferromagnet with a little axial anisotropy, which is the case here,<sup>1</sup> and the beginning contribution of phonon scattering, and reminds us of the low- $T$  behavior of pure Gd measured by Lüthi and Rohrer,<sup>19</sup> with a  $T^{3.1}$  dependence for the magnetic and a  $T^{3.5-3.8}$  dependence for the phonon part. The decreasing resistivity slope for the H-loaded specimens just before the hump near 4 K (cf. Fig. 3) is an indication of further loss of anisotropy, a suggestion to be confirmed by neutron scattering. This and the increasing absolute value of  $\rho_0$  with increasing  $x$  are clear signs for the presence of a superimposed AF magnetism of  $\text{GdH}_2$ .

Hence, the analysis of the electrical resistivity of the hydrogen-doped alloy  $\text{Y}_{0.4}\text{Gd}_{0.6}\text{H}(\text{D})_x$  has led to the following principal conclusions.

(i) The quasi-invariable residual resistivity at all studied  $x$

values, the absence of an anomaly near 170 K which could have been indicative of H-sublattice ordering, and the absence of any isotope effect are a sign for a nonexisting low-temperature  $\alpha^*$ -solid solution phase. This is in agreement with the suggested correlation between the presence of an  $\alpha^*$  phase and the value for the interlayer turn angle  $\omega_i$  of the modulated magnetic configuration.

(ii) The values of the antiferromagnetic  $T_N^{\text{Gd}}$  at 192 K and of the ferromagnetic  $T_C^{\text{Gd}}$  at 80 K remain practically unchanged by H addition but the amplitudes of their manifestations are rather weakened.

(iii) The paramagnetic spin-disorder resistivity and the related  $\rho$  slope in the linear range below  $T_N^{\text{Gd}}$  decrease with increasing  $x$ .

(iv) Hydrogen precipitates as  $\text{GdH}_2$  for the lowest employed  $x$  values, which is seen as a superimposed hump at  $T = 3.6$  K upon the resistivity of the pure alloy. This  $T_N^{\text{GdH}_2}$  is much smaller than that of bulk  $\text{GdH}_2$  ( $T_N = 18.5$  K), indicating a strong interaction between the different domains, also seen on the spin-wave spectrum.

A qualitative neutron-scattering analysis of this system is indicated and programmed.

<sup>1</sup>B. Coqblin, *Electronic Structure of Rare-earth Metals and Alloys* (Academic, New York, 1977).

<sup>2</sup>A. V. Andrianov, *J. Magn. Magn. Mater.* **140/144**, 749 (1995); A. V. Andrianov and O. D. Chistiakov, *Phys. Rev. B* **55**, 14 107 (1997).

<sup>3</sup>R. Griessen *et al.*, *J. Alloys Compd.* **253/4**, 44 (1997); P. van der Sluis, M. Ouwerkerk, and P. A. Duine, *Appl. Phys. Lett.* **70**, 3356 (1997).

<sup>4</sup>P. Vajda, in *Handbook on the Physics and Chemistry of Rare Earths*, edited by K. A. Gschneidner (North-Holland, Amsterdam, 1995), Vol. 20, p. 207.

<sup>5</sup>P. Vajda and O. J. Zogal, *Phys. Rev. B* **59**, 9467 (1999).

<sup>6</sup>P. Vajda, *8th International Conference on  $\mu\text{SR}$*  (Les Diablerets, Suisse, 1999); *Physica B* (to be published).

<sup>7</sup>H. M. Fretwell *et al.*, *Phys. Rev. Lett.* **82**, 3867 (1999).

<sup>8</sup>W. C. Thoburn, S. Legvold, and F. H. Spedding, *Phys. Rev.* **110**, 1298 (1958).

<sup>9</sup>D. M. S. Bagguley, J. Liesegang, and K. Robinson, *J. Phys. F:*

*Met. Phys.* **4**, 594 (1974).

<sup>10</sup>J. Hennepf, *Phys. Lett.* **11**, 273 (1964).

<sup>11</sup>T. Sugawara, *J. Phys. Soc. Jpn.* **20**, 2252 (1965).

<sup>12</sup>H. R. Child and J. W. Cable, *J. Appl. Phys.* **40**, 1003 (1969).

<sup>13</sup>S. Bates *et al.*, *Phys. Rev. Lett.* **55**, 2968 (1985).

<sup>14</sup>M. Foldeaki, R. Chahine, and T. K. Bose, *Phys. Rev. B* **52**, 3471 (1995).

<sup>15</sup>P. Vajda, J. N. Daou, A. Lucasson, and J. P. Burger, *J. Phys. F: Met. Phys.* **17**, 1029 (1987); M. W. McKergow, D. K. Ross, J. E. Bonnet, I. S. Anderson, and O. Schaerpf, *J. Phys. C* **20**, 1909 (1987).

<sup>16</sup>P. Vajda, J. P. Burger, and J. N. Daou, *J. Phys.: Condens. Matter* **3**, 6267 (1991).

<sup>17</sup>S. B. Dugdale *et al.*, *Phys. Rev. Lett.* **79**, 941 (1997).

<sup>18</sup>P. Vajda, J. N. Daou, and J. P. Burger, *J. Less-Common Met.* **172/4**, 271 (1991).

<sup>19</sup>R. Lüthi and H. Rohrer, *Solid State Commun.* **3**, 257 (1965).